

ELF Generation in the Lower Ionosphere via Collisional Parametric Decay

K. KO,¹ C. R. MENYUK,¹ A. REIMAN,² V. TRIPATHI,³
P. PALMADESSO,⁴ AND K. PAPAPOPOULOS⁵

Generation of ELF waves by stimulated parametric coupling of two HF waves in the lower ionosphere is considered. In this region the nonlinear force is dominated by the thermal rather than the ponderomotive nonlinearity. It is shown that this results in lowering the pump threshold for complete decay by more than an order of magnitude while achieving efficiencies in excess of those expected on the basis of the Manley-Rowe relations. The lower-frequency mode excited for E region altitudes is the helicon mode, which continues to frequencies below the ion cyclotron frequency because ion-neutral collisions freeze the ion motion. The application of these results to ELF generation in the lower ionosphere, including power estimates for a proof of principle experiment, is discussed.

1. INTRODUCTION

The interaction of high-power radio waves with the ionospheric plasma is strongly nonlinear. The main nonlinearities arise through the ponderomotive and thermal forces. As a result of the nonlinear interactions, electrostatic (es) and electromagnetic (em) waves with frequencies different from the pump frequency can be generated. A comprehensive review of the subject can be found in a recent monograph [Gurevich, 1978]. The present paper examines the feasibility and the efficiency of utilizing the nonlinearities of the ionospheric plasma to downconvert HF signals to ELF in a controlled fashion. The subject matter, besides its intrinsic scientific merit, has a broad spectrum of applications, ranging from ionospheric and magnetospheric probing to low-frequency submarine communications. The emphasis in this work will be on the nonlinear physics aspects of the interaction, the projected scalings, and the heater requirements for a proof of principle experiment.

Ionospheric heaters have been used successfully for the generation of VLF and ULF signals [Stubbe and Kopka, 1977; Stubbe *et al.*, 1981; Ferraro *et al.*, 1982]. These experiments induced local modulation of existing ionospheric currents, such as the auroral and equatorial electrojets, by illuminating the current-carrying region with strong HF waves amplitude-modulated at the desired low frequency. The basic physics of the technique, known as nonlinear demodulation or, for historical reasons, ionospheric detection, lies in the fact that the HF wave produces modulated electron heating, which results in modulation of the local conductivity. Natural ionospheric currents which pass through the illuminated region are modulated by the conductivity changes, producing a radiating dipole current pattern [Chang *et al.*, 1981]. The radiated low-frequency wave couples to the earth-ionosphere waveguide and propagates to long distances with small attenuation [Chang *et al.*, 1981]. The earliest experimental results on nonlinear demodulation were observed during the Soviet heating

experiments at Gorki [Germantsev *et al.*, 1974; Kapustin *et al.*, 1977]. The polar electrojet was modulated in the VLF range (1–7 kHz) with a 5.75-MHz carrier and 15-MW effective radiative power (ERP). Signals were observed only between 2.5 and 4 kHz with strength in the range $2\text{--}25 \times 10^{-2} \mu\text{V/m}$. More reliable results for polar electrojet modulation were reported by the Max Planck group [Stubbe *et al.*, 1982a, b] using the Tromso Norway ionospheric heater. The ERP in this case varied between 75 and 125 MW, and the HF frequency utilized was 2.5–8 MHz. VLF signals with amplitude $10^{-3} \gamma$ were observed with maxima for 2 kHz. Finally, Ferraro *et al.* [1982] reported VLF signals in the 500-Hz to 5-kHz range using the Arecibo HF heater at 3.17 MHz to modulate the equatorial electrojet. Again maximum strength appeared for 2-kHz VLF signals.

Because of technical problems with the Tromso heating facility it has not been possible to generate signals in the 10-Hz to 200-Hz regime. However, signals up to 10 γ have been generated for Pc 5 pulsations up to 10 Hz. These signals are much larger than expected from current modulation, and their physical origin has been a mystery. In a recent paper, Papadopoulos and Chang [1985] noted that spontaneously generated magnetic fields with time variation similar to the HF modulation can be generated during ionospheric heating experiments when $\nabla n \times \nabla T_e \neq 0$, where ∇n is the ambient ionospheric density gradient and ∇T_e the electron temperature gradient in the heated region. The generation of these fields is independent of the ambient current, and its physical origin has been demonstrated in laser-produced plasmas [Stamper *et al.*, 1971]. Papadopoulos and Chang [1985] indicate that for frequencies below 40 Hz the spontaneous field generation dominates over the current modulation, thereby explaining the large observed signals.

While the above mechanisms appear to be rather well understood, they are relatively inefficient in downconverting HF power to ELF. In addition the nonlinear demodulation can be applied only in regions of preexisting currents, and the maximum generated signal amplitude is strictly constrained by the local current values. These limitations provoked the search for other more efficient nonlinear mechanisms for ELF generation which are independent of the ambient current. Papadopoulos *et al.* [1982] considered the possibility of parametric excitation of an Alfvén or magnetosonic wave in the ionosphere by beating two high-frequency waves (ω_1, ω_2) with $\omega_1 - \omega_2$ equal to the frequency of the low-frequency mode (ω_3). The process envisioned was essentially a modified stimulated for-

¹Science Applications International Corporation, McLean, Virginia.

²Princeton Plasma Physics Laboratory, Princeton, New Jersey.

³Indian Institute of Technology, New Delhi, India.

⁴Naval Research Laboratory, Washington, D. C.

⁵University of Maryland, College Park.

Copyright 1986 by the American Geophysical Union.

Paper number 5A8524.
0148-0227/86/005A-8524\$05.00

ward Brillouin scattering [Liu, 1976] with the Alfvén wave, instead of an ion acoustic wave, acting as the low-frequency signal. In the language of parametric instabilities the pump (ω_1) and the idler (ω_2) are HF waves, while the signal (ω_3) was an Alfvén or magnetosonic mode. In the work by Papadopoulos *et al.* [1982] the process was considered as collisionless so that the ponderomotive force was the dominant nonlinear force. The power threshold necessary for complete decay can be found by the inverse scattering transform (IST) method [Zakharov and Manakov, 1975; Reiman, 1977; Kaup *et al.*, 1979]. The analysis revealed that for upper *F* region ionospheric parameters the power threshold necessary to excite Alfvén waves was very large. In addition the maximum down-conversion efficiency was limited by the Manley-Rowe relations [Sagdeev and Galeev, 1969] to ω_3/ω_1 , i.e., less than 10^{-4} for downconverting 5 MHz to 100 Hz. It was subsequently noted [Papadopoulos *et al.*, 1983] that if the thermal nonlinearity caused by collisional electron heating [Berger *et al.*, 1975; Gurevich, 1978] dominates over the ponderomotive force, the downconversion efficiency is increased by a factor v/ω_3 where v is the electron collision frequency. Furthermore, the power threshold required for complete decay is reduced by a comparable v/ω_3 factor. Since the values of v are larger for the lower ionosphere (i.e., *E* region), it is advantageous to consider the interaction in this region.

In this paper we examine the ELF generation in the ionospheric *E* region by the beating of two HF heaters. In the next section we discuss the ELF plasma eigenmodes in the *E* region where the two HF pumps will couple and derive the equations describing the nonlinear interaction of the three wave packets. It is noted that for altitudes below 150 km the ion-neutral collision frequency (ν_3) is larger than the ion cyclotron frequency (ω_{ci}), thereby not allowing the existence of proper Alfvén or magnetosonic eigenmodes. It is then found that the viscous ion damping ($\nu_3 > \omega_{ci}$) freezes the ion motion and allows the whistler mode to continue as a helicon [Aigrain, 1961], a right-hand polarized mode, to frequencies $\omega_3 < \nu_3$. In section 3 we extend the work performed on threshold conditions and power transfer efficiency in collisionless three-wave packet interactions to the collisional regime. This section includes many novel and rather profound physical issues. Section 4 uses the mathematical and numerical conclusions of section 3 to compute the power and electric field threshold conditions for ELF generation in the lower ionosphere by two HF pumps under steady state conditions and to discuss the antenna requirements for a proof of principle experiment. The final section summarizes our results, stresses their limitations, and outlines potential improvements and extensions.

2. NONLINEAR INTERACTION OF TWO HF WAVE PACKETS WITH AN ELF WAVE IN THE LOWER IONOSPHERE

We assume first that the two interacting high-frequency waves have $\omega_1, \omega_2 \gg \omega_{ce}$, where ω_{ce} is the electron cyclotron frequency. In this case the plasma behaves isotropically, so that the dielectric tensors $\epsilon_{1,2}$ of the two waves are diagonal, i.e., $\epsilon_{1,2}$ are diagonal. In the fluid approximation the dispersion relation is then

$$D_{1,2} = \frac{\omega_{1,2}^2}{c^2} \epsilon_{1,2} - k_{1,2}^2 = 0 \quad (1a)$$

$$\epsilon_{1,2} = 1 - \frac{\omega_{pe}^2}{\omega_{1,2}^2} \left[1 - \frac{iv}{\omega_{1,2}} \right] \quad (1b)$$

where ω_{pe} is the plasma frequency and ν the electron-neutral collision frequency. For the low-frequency wave we consider, $\omega_3 < \omega_{pi}$, where ω_{pi} is the ion plasma frequency, so that we can neglect its electric field parallel to the ambient magnetic field, whose direction is taken along the *z* axis (i.e., $E_{3z} \approx 0$). The dispersion relation for the low-frequency wave is then [Krall and Trivelpiece, 1973]

$$\begin{bmatrix} \frac{\omega_3^2}{c^2} \epsilon_3^{xx} - k_{3z}^2 & \frac{\omega_3^2}{c^2} \epsilon_3^{xy} \\ -\frac{\omega_3^2}{c^2} \epsilon_3^{xy} & \frac{\omega_3^2}{c^2} \epsilon_3^{xx} - k_3^2 \end{bmatrix} = 0 \quad (2)$$

where ϵ_3^{xx} and ϵ_3^{xy} are the diagonal and the off-diagonal elements of the cold plasma dielectric tensor. Assuming $\omega_{ce} \gg \nu \gg \omega_3$, we find

$$\epsilon_3^{exx} = \frac{i\omega_{pe}^2}{\omega_{ce}^2} \frac{\omega_3}{\nu} \quad \epsilon_3^{exy} = -\frac{i\omega_{pe}^2}{\omega_{ce}\omega_3} \quad (3a)$$

$$\epsilon_3^{ixx} = \frac{\omega_{pi}^2(\omega_3 + iv_3)}{\omega_3[\omega_{ci}^2 - (\omega_3 + iv_3)^2]} \quad (3b)$$

$$\epsilon_3^{ixy} = \frac{i\omega_{pi}^2\omega_{ci}}{\omega_3[\omega_{ci}^2 - (\omega_3 + iv_3)^2]}$$

For $\omega_{pi} > \nu$, $\max(\omega_{ci}, \nu_3, \omega_3)$, equations (3) reduce to

$$\epsilon_3^{xx} = 1 + \epsilon_3^{exx} + \epsilon_3^{ixx} = \frac{\omega_{pi}^2}{[\omega_{ci}^2 - (\omega_3 + iv_3)^2]} \frac{\omega_3 + iv_3}{\omega_3} \quad (4a)$$

$$\epsilon_3^{xy} = \epsilon_3^{exy} + \epsilon_3^{ixy} = -\frac{i\omega_{pe}^2}{\omega_{ce}\omega_3} \left[1 - \frac{(\omega_3 + iv_3)^2}{\omega_{ci}^2} \right]^{-1} \quad (4b)$$

From (2) and (4) and neglecting the displacement current we find the following regimes of weakly attenuated proper eigenmodes: (1) For $\omega_{ci} \gg \omega_3, \nu_3$,

$$\epsilon_3^{xx} = \frac{\omega_{pi}^2}{\omega_{ci}^2} \left(1 + \frac{iv_3}{\omega_3} \right) \quad (5a)$$

$$\epsilon_3^{xy} = 0 \quad (5b)$$

which allows propagation of Alfvén waves as long as $\nu_3/\omega_3 \ll 1$. (2) For $\omega_3 \gg \omega_{ci}, \nu_3$,

$$\epsilon_3^{xx} = 0 \quad (6a)$$

$$\epsilon_3^{xy} = -\frac{i\omega_{pe}^2}{\omega_{ce}\omega_3} \quad (6b)$$

which is the usual electron whistler. (3) For $\nu_3 \gg \omega_{ci}, \omega_3$,

$$\epsilon_3^{xx} = 0 \quad (7a)$$

$$\epsilon_3^{xy} = -\frac{i\omega_{pe}^2}{\omega_{ce}\omega_3} \quad (7b)$$

regardless of the ω_3/ω_{ci} ratio. This is similar to the whistler dispersion found above for $\omega_3 > \omega_{ci}$; it is the helicon mode (C. R. Menyuk and K. Papadopoulos, private communication, 1984). In this case, contrary to case 1 above, the current is carried by the electrons while the ions are viscously frozen. In this sense it is analogous to the well-known helicon wave in solid-state physics [Aigrain, 1961] in which the current is carried by the free electrons, while the ion motion is frozen by the lattice. Referring to the excitation of ELF waves below 100 Hz

in the lower ionosphere, it is obvious that the relevant mode is the helicon rather than the Alfvén mode, to which we shall restrict our attention.

Our starting point for the derivation of the nonlinear currents that couple the three modes is the warm collisional electron fluid equations [Gurevich, 1978; Perkins and Goldman, 1981]

$$\left[\frac{\partial}{\partial t} + \mathbf{v}_e \cdot \nabla \right] \mathbf{v}_e = -\frac{e}{m_e} \left[\mathbf{E} + \frac{\mathbf{v}_e \times \mathbf{B}}{c} \right] - \nu \mathbf{v}_e - \frac{\nabla p_e}{m_e n_e} \quad (8)$$

$$\left[\frac{\partial}{\partial t} + \mathbf{v}_e \cdot \nabla \right] n_e = -n_e \nabla \cdot \mathbf{v}_e \quad (9)$$

$$\left[\frac{\partial}{\partial t} + \mathbf{v}_e \cdot \nabla \right] T_e = \frac{2}{3} (\nu m_e \mathbf{v}_e - T_e \nabla) \cdot \mathbf{v}_e - \Delta v (T_e - T_0) \quad (10)$$

which together with the equation of state for the pressure, $p_e = n_e T_e$, form a closed system of equations for n_e , \mathbf{v}_e , and T_e ; Δv is the mean fraction of energy lost per collision, and T_0 the ambient temperature. In (10) we have neglected heat conduction, an assumption valid for the E but not for the F region. Other terms neglected, such as friction and thermal force, do not change the final results. The nonlinear currents can be computed by considering small perturbations about a non-drifting equilibrium (n_0 , T_0) so that $\mathbf{v}_e = \mathbf{v}$, $n_e = n_0 + n$, and $T_e = T_0 + T$, assuming plane wave solutions of the form $\exp[-i(\omega \cdot t - \mathbf{k} \cdot \mathbf{r})]$ and using the resonance conditions

$$\omega_1 = \omega_2 + \omega_3 \quad (11)$$

$$\mathbf{k}_1 = \mathbf{k}_2 + \mathbf{k}_3$$

The computation is tedious but straightforward and is given in the appendix. The resulting high-frequency nonlinear currents are

$$\mathbf{J}_1^{NL} = -\frac{e}{4\pi m_e \omega_2} \left(1 - \frac{i\nu}{\omega_2} \right) (\mathbf{k}_3 \cdot \boldsymbol{\varepsilon}_3^e \cdot \mathbf{E}_3) \quad (12)$$

$$\mathbf{J}_2^{NL} = \frac{e}{4\pi m_e \omega_1} \left(1 - \frac{i\nu}{\omega_1} \right) (\mathbf{k}_3 \cdot \boldsymbol{\varepsilon}_3^e \cdot \mathbf{E}_3)^*$$

Here and in the rest of the paper, \mathbf{v} , n , T , \mathbf{J} , and \mathbf{E} are Fourier-transformed quantities. With the exception of the small $i\nu/\omega_{1,2}$ terms, (12) is the standard result [Weiland and Wilhelmsson, 1977]. The low-frequency nonlinear current is given by

$$\mathbf{J}_3^{NL} = \frac{e}{4\pi m_e \omega_1 \omega_2} \boldsymbol{\varepsilon}_3^e \cdot \mathbf{k}_3 (\mathbf{E}_1 \cdot \mathbf{E}_2^*) \left(1 + \frac{i4\nu}{3\omega_3} \right) \quad (13)$$

For $\nu = 0$ this is again nothing more than the standard low-frequency current caused by the collisionless ponderomotive force [Papadopoulos et al., 1982]. The coefficient $4\nu/3\omega_3$ is due to the nonlinear perturbation caused by ohmic heating. For $\nu/\omega_3 \gg 1$ it becomes the dominant term, introducing a ν/ω_3 enhancement factor in the current as well as a $\pi/2$ phase shift. Several physical comments on the derivation of (12) and (13) can be found in the appendix.

Using the currents \mathbf{J}^{NL} as a source in the wave equation for each of the three waves, we find

$$\mathbf{D}_j \cdot \mathbf{E}_j = -\frac{i4\pi\omega_j}{c^2} \mathbf{J}_j^{NL} \quad (14)$$

$$\mathbf{D}_j = \frac{\omega_j}{c^2} \boldsymbol{\varepsilon}_j - k_j^2 \mathbf{I} + \mathbf{k}_j \mathbf{k}_j$$

In the absence of nonlinear currents ($\mathbf{J}^{NL} = 0$) the vanishing of the determinants, $|\mathbf{D}| = 0$, represents the linear dispersion relations of the individual waves, which were given by (1) and (2). Taking without loss of generality the polarizations of $\mathbf{E}_{1,2}$ as

$$\mathbf{E}_{1,2} = E_{1,2} \mathbf{y} \quad (15)$$

and using the isotropic property of the tensors $\boldsymbol{\varepsilon}_{1,2}$ for $\omega_{1,2} \gg \omega_{ce}$, we find

$$D_1 E_1 = -\frac{i4\pi\omega_1}{c^2} J_1^{NL} \quad (16)$$

$$D_2 E_2 = -\frac{i4\pi\omega_2}{c^2} J_2^{NL}$$

with $D_{1,2}$ given by (1) and $J_{1,2}^{NL}$ by (12). For the polarization given by (15) and using the fact that $E_{3z} \approx 0$ for $\omega_3 \ll \omega_{pi}$, the equations for the low-frequency wave are given by

$$\left[\frac{\omega_3^2}{c^2} \boldsymbol{\varepsilon}_3^{xx} - k_{3z}^2 \right] E_{3x} + \frac{\omega_3^2}{c^2} \boldsymbol{\varepsilon}_3^{xy} E_{3y} = -\frac{i4\pi\omega_3}{c^2} J_{3x}^{NL} \quad (17a)$$

$$-\frac{\omega_3^2}{c^2} \boldsymbol{\varepsilon}_3^{xy} E_{3x} + \left[\frac{\omega_3^2}{c^2} \boldsymbol{\varepsilon}_3^{xx} - k_{3z}^2 \right] E_{3y} = -\frac{i4\pi\omega_3}{c^2} J_{3y}^{NL} \quad (17b)$$

where $\boldsymbol{\varepsilon}_3^{xx}$ and $\boldsymbol{\varepsilon}_3^{xy}$ are given by (4). Eliminating E_{3x} from (17), we find

$$D_3 E_{3y} = -\frac{i4\pi\omega_3}{c^2} \left[\frac{\omega_3^2}{c^2} \boldsymbol{\varepsilon}_3^{xy} \left[\frac{\omega_3^2}{c^2} \boldsymbol{\varepsilon}_3^{xx} - k_{3z}^2 \right]^{-1} \cdot J_{3x}^{NL} + J_{3y}^{NL} \right] \quad (18)$$

where

$$D_3 = \left[\frac{\omega_3^2}{c^2} \boldsymbol{\varepsilon}_3^{xy} \right]^2 \left[\frac{\omega_3^2}{c^2} \boldsymbol{\varepsilon}_3^{xx} - k_{3z}^2 \right]^{-1} + \left[\frac{\omega_3^2}{c^2} \boldsymbol{\varepsilon}_3^{xx} - k_{3z}^2 \right] \quad (19)$$

Depending on whether we are coupling to Alfvén waves or whistler-helicon waves, the values of the dielectric tensor elements will be given by (5) or (7). In this paper we are interested in coupling to helicons, so that

$$\frac{|\boldsymbol{\varepsilon}_3^{xy}|}{\boldsymbol{\varepsilon}_3^{xx}} = \frac{m_i}{m_e} \frac{\nu}{\omega_{ce}} \gg 1$$

Therefore D_3 becomes

$$D_3 = -\frac{[k_3 k_{3z} - (\omega_3^2/c^2) |\boldsymbol{\varepsilon}_3^{xy}|] [k_3 k_{3z} + (\omega_3^2/c^2) |\boldsymbol{\varepsilon}_3^{xy}|]}{k_3^2} \quad (20)$$

with $\boldsymbol{\varepsilon}_3^{xy}$ given by (7b). The case of Alfvén waves can be examined in an analogous manner. Assuming without loss of generality that $k_{3y} = 0$, we find that

$$\mathbf{k}_3 \cdot \boldsymbol{\varepsilon}_3 \cdot \mathbf{E}_3 = k_{3x} \boldsymbol{\varepsilon}_3^{xy} E_{3y}$$

so that $\mathbf{J}_3 = J_{3y} \mathbf{y}$. From (12), (13), (16), (18), and (20) we find the coupled system of equations,

$$D_1 \frac{E_1}{\omega_1} = \beta \left(1 - \frac{i\nu}{\omega_2} \right) \frac{E_2 E_3}{\omega_2 \omega_3} \quad (21a)$$

$$D_2 \frac{E_2}{\omega_2} = \beta \left(1 - \frac{iv}{\omega_1} \right) \frac{E_1 E_3^*}{\omega_1 \omega_3} \quad (21b)$$

$$D_3 \frac{E_3}{\omega_3} = \beta \left(1 + \frac{i4v}{3\omega_3} \right) \frac{E_1 E_2^*}{\omega_1 \omega_2} \quad (21c)$$

where

$$\beta = \frac{e}{m_e c^2} \frac{k_{3x} \omega_{pe}^2}{\omega_{ce}} \quad (22)$$

and we have set $E_{3y} = E_3$. In the collisionless case the high-frequency waves produce a low-frequency ponderomotive force acting on the electrons, which results in a nonlinear current J^{NL} that drives E_3 . In the collisional case, J^{NL} is predominantly due to a low-frequency temperature perturbation T^{NL} when the electrons are ohmically heated. In either case, the beating of the high-frequency velocities $\mathbf{v}_1, \mathbf{v}_2$ with the low-frequency density perturbation n_3 (see appendix) provides the primary coupling mechanism between E_3 and the high-frequency fields E_1, E_2 . It is worth noting that by choosing the HF electric field polarization in the y direction in the interaction with $\omega_3 \ll \omega_1, \omega_2, |\mathbf{k}_3| \ll |\mathbf{k}_1|, |\mathbf{k}_2|$, we end up with all of the nonlinear currents and the low-frequency electric field in the y direction.

Equations (21) describe the interaction of infinite, homogeneous, plane waves. In practice, however, we deal with two HF wave packets interacting with an ELF wave packet within a spatially localized region controlled by the antenna gain. In order to determine the efficiency of the interaction the localized and inhomogeneous nature of the wave packet should be included. For a weakly nonlinear interaction between localized wave packets, we follow the standard procedure and expand D_j in a Taylor series about the phase matching point where the resonance conditions (11) are met; that is, we let

$$D_j + \frac{i\partial D_j}{\partial \omega_j} \left[\frac{\partial}{\partial t} + \Gamma_j \right] - \frac{i\partial D_j}{\partial \mathbf{k}_j} \cdot \nabla + \dots$$

operate on

$$E_j(\mathbf{r}, t) = \mu_j a_j(\mathbf{r}, t) \exp[-i(\omega_j t - \mathbf{k}_j \cdot \mathbf{r})] \quad (23a)$$

where

$$\mu_j = \omega_j / (\partial D_j / \partial \omega_j)^{1/2} \quad (23b)$$

and a_j is the slowly varying envelope of the j th wave packet. The linear damping rates Γ_j are given by the imaginary parts of D_j while the partial derivatives of D_j are evaluated for a particular mode (ω_j, \mathbf{k}_j) . For positive energy waves, as is the case here, $\partial D_j / \partial \omega_j > 0$. Using the fact that to lowest order, the waves obey the linear dispersion relations $D_j = 0$, we obtain the equations for the collisional three-wave coupling in standard form:

$$\left(\frac{\partial}{\partial t} + \mathbf{u}_1 \cdot \nabla + \Gamma_1 \right) a_1 = K \left(1 - \frac{iv}{\omega_2} \right) a_2 a_3 \quad (24a)$$

$$\left(\frac{\partial}{\partial t} + \mathbf{u}_2 \cdot \nabla + \Gamma_2 \right) a_2 = -K^* \left(1 - \frac{iv}{\omega_1} \right) a_1 a_3^* \quad (24b)$$

$$\left(\frac{\partial}{\partial t} + \mathbf{u}_3 \cdot \nabla + \Gamma_3 \right) a_3 = -K^* \left(1 + \frac{i4v}{3\omega_3} \right) a_1 a_2^* \quad (24c)$$

where

$$\mathbf{u}_j = - \frac{\partial D_j}{\partial \omega_j} \left(\frac{\partial D_j}{\partial \mathbf{k}_j} \right)^{-1} \quad (25a)$$

are the group velocities of the waves and

$$K = -i\beta \left(\frac{\partial D_1 \partial D_2 \partial D_3}{\partial \omega_1 \partial \omega_2 \partial \omega_3} \right)^{-1/2} \quad (25b)$$

is the symmetric coupling coefficient for the collisionless interaction. By setting $\partial/\partial t = 0$, one finds the steady state two-dimensional version,

$$\left(\frac{\partial}{\partial z} + \tilde{u}_1 \frac{\partial}{\partial x} + \tilde{\Gamma}_1 \right) \tilde{a}_1 = \tilde{K} \left(1 - \frac{iv}{\omega_2} \right) \tilde{a}_2 \tilde{a}_3 \quad (26a)$$

$$\left(\frac{\partial}{\partial z} + \tilde{u}_2 \frac{\partial}{\partial x} + \tilde{\Gamma}_2 \right) \tilde{a}_2 = -\tilde{K}^* \left(1 - \frac{iv}{\omega_1} \right) \tilde{a}_1 \tilde{a}_3^* \quad (26b)$$

$$\left(\frac{\partial}{\partial z} + \tilde{u}_3 \frac{\partial}{\partial x} + \tilde{\Gamma}_3 \right) \tilde{a}_3 = -\tilde{K}^* \left(1 + \frac{i4v}{3\omega_3} \right) \tilde{a}_1 \tilde{a}_2^* \quad (26c)$$

where the interaction is assumed to evolve in z ($u_{jz} > 0$). The new variables are expressed as follows:

$$\tilde{a}_j = a_j u_{jz}^{1/2} \quad \tilde{u}_j = u_{jx}/u_{jz} \quad \tilde{\Gamma}_j = \Gamma_j/u_{jz} \quad (27a)$$

$$\tilde{K} = K/(u_{1z} u_{2z} u_{3z})^{1/2} \quad (27b)$$

Equations (26) with the definitions from (23) and (25), the value of β given by (22), and D_1, D_2, D_3 from (1) and (20) form the basic equations of our problem. In the next section we will use them to determine the transfer efficiency during the steady state interaction of the three wave packets.

3. THRESHOLD CONDITIONS AND TRANSFER EFFICIENCY FOR THREE-WAVE PACKET INTERACTIONS IN DISSIPATIVE SYSTEMS

Before attempting to solve (26) for the situation under study, it is worthwhile to review briefly the previous work on the subject, which, owing to its rather mathematical nature, might not have reached the ionospheric community. In the collisionless case (i.e., $v = 0$), the coupling coefficients are symmetric, and the set of equations (24) has an infinite set of invariants. This allows for the use of inverse scattering transform (IST) techniques [Ablowitz and Segur, 1981]. The one-dimensional version of (24) [Zakharov and Manakov, 1975; Reiman, 1977; Kaup et al., 1979] has been extensively studied in the literature using IST, and the results were confirmed by numerical solutions. As noted before, the two-dimensional steady state equations (26) are equivalent to the transformed one-dimensional space-time equations. Therefore the results of the one-dimensional space-time problem can be directly applied to our practical problem. An important result of the one-dimensional space-time collisionless analysis is the fact that the threshold value required for pump depletion is equivalent to the pump amplitude required to achieve an absolute instability within its width L [Reiman, 1977].

For collisionless three-wave interactions, the eigenvalue problem which determines the conditions for absolute instability in a rectangular pump is well known (i.e., the backward wave oscillator) [Bobroff and Haus, 1967]. Taking the pump inhomogeneity to be along x , the instability is absolute if

$$u_{2x} u_{3x} < 0 \quad (28a)$$

$$L > \frac{\pi}{2} L_c \quad (28b)$$

where $L_c = |u_{2x} u_{3x}|^{1/2} / |\gamma_0|$ is the critical width and $|\gamma_0| = |K^* a_1|$ is the uniform medium growth rate. Equation (28a) requires the decay waves to be oppositely traveling, while

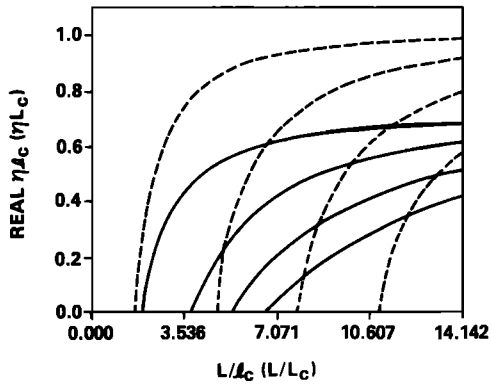


Fig. 1a. Real part of ηl_c (ηL_c) versus L/l_c (L/L_c) for the collisional (collisionless) interaction. The dotted lines refer to the collisionless case.

equation (28b) defines the pump threshold for the absolute instability to occur within a width L . We demonstrate below that for the strongly collisional case ($\nu/\omega_3 \gg 1$), similar considerations apply. Note that, however, since the coupling coefficients are by a factor ν/ω_3 larger, the required pump levels are smaller by the same factor. In addition the transfer efficiency increases by the same factor. Notice that because of the dissipative nature of the system, IST techniques are not applicable, so that one has to resort to numerical techniques.

The linear equations for the eigenvalue problem that determine absolute instability when one considers the initial stage of the interaction during which the pump is large, $a_1 \gg a_2, a_3$, are given by the one-dimensional version of (24b) and (24c). Here only the evolution of the decay waves is important, so that we have

$$\left(\frac{\partial}{\partial t} + u_{2x} \frac{\partial}{\partial x} + \Gamma_2 \right) a_2 = -\gamma_0(x) a_3 \left(1 - \frac{i\nu}{\omega_1} \right) \quad (29a)$$

$$\left(\frac{\partial}{\partial t} + u_{3x} \frac{\partial}{\partial x} + \Gamma_3 \right) a_3 = -\gamma_0(x) a_2 \Lambda \quad (29b)$$

Note that $\gamma_0(x)$ contains the pump inhomogeneity and Λ is defined by

$$\Lambda = 1 + \frac{i4\nu}{3\omega_3} \quad (30)$$

For the threshold calculation here, we can ignore the small collisional correction on the right-hand side of (29a). The linearly coupled system is solved by taking the conjugate of (29a) and Laplace transforming in time as e^{pt} . We then make the substitution

$$(a_2^*, a_3) = \exp \left[-\frac{1}{2} \left(\frac{p + \Gamma_2}{u_{2x}} + \frac{p + \Gamma_3}{u_{3x}} \right) x \right] (A_2, A_3) \quad (31)$$

to obtain

$$\left(\frac{\partial}{\partial x} + \eta \right) A_2 = -\frac{\gamma_0^*(x)}{u_{2x}} A_3 \quad (32a)$$

$$\left(\frac{\partial}{\partial x} - \eta \right) A_3 = -\frac{\gamma_0(x)}{u_{3x}} A_2 \Lambda \quad (32b)$$

where

$$\eta = \frac{1}{2} \left(\frac{p + \Gamma_2}{u_{2x}} - \frac{p + \Gamma_3}{u_{3x}} \right) \quad (33)$$

Equations (32), when subject to the appropriate boundary conditions, form the eigenvalue problem for the growth rate p which may in general be complex.

In the case of a rectangular pump of width L ,

$$\gamma_0(x) = \gamma_0 \quad -L/2 \leq x \leq L/2$$

$$\gamma_0(x) = 0 \quad \text{otherwise}$$

one may combine (32) inside the pump region to find

$$\left(\frac{\partial^2}{\partial \zeta^2} + q \right) A_3 = 0 \quad (34)$$

which describes a harmonic oscillator in the normalized coordinate $\zeta = x/l_c$ with a potential

$$q = e^{i\theta} - \eta^2 l_c^2$$

where

$$\theta = \tan^{-1} \left(\frac{4\nu}{3\omega_3} \right)$$

The new critical width is given by

$$l_c = L_c / |\Lambda|^{1/2} \quad (35)$$

Equation (34) readily admits solutions in terms of trigonometric functions to which we apply the boundary conditions that A_3 be zero at $-L/2$ and A_3 be zero at $L/2$ for $u_{2x} > 0$, $u_{3x} < 0$. This leads to the dispersion relation

$$q^{1/2} \cot(q^{1/2} L_c / l_c) + \eta l_c = 0 \quad (36)$$

for the normalized growth rate ηl_c . We have evaluated (36) numerically in the limit $\nu/\omega_3 \gg 1$, which sets $\theta = \pi/2$ and $|\Lambda| \sim \nu/\omega_3$. Complex eigenvalues are found, which indicates that absolute instability indeed occurs in the collisional regime. The real and imaginary parts of ηl_c for the first four growing modes are shown in Figures 1a and 1b as a function of the normalized width L/l_c . For comparison, the results for the collisionless regime ($\nu = 0$; $\theta = 0$, $\Lambda = 1$, $l_c \rightarrow L_c$) are also plotted; in this case, the growth rates are purely real. From Figure 1a, one finds the threshold condition in the collisional regime to be

$$L > 1.8 l_c \quad (37)$$

For a given width L it is clear that the pump value a_1 required to achieve absolute instability for the collisional interaction is smaller by the factor $l_c/L_c = |\Lambda|^{-1/2}$. Thus a reduction in the

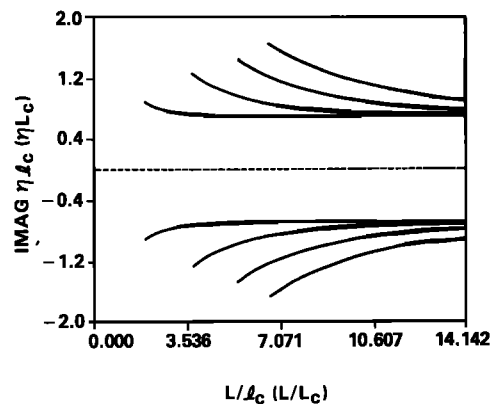


Fig. 1b. Imaginary part of ηl_c (ηL_c) versus L/l_c (L/L_c) for the collisional (collisionless) interaction. The dotted line at zero is for the collisionless case.

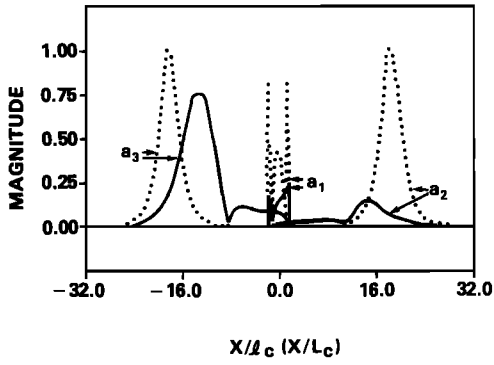


Fig. 2. Wave profiles at $t = 25.0$ for the collisional (solid lines) and collisionless (dotted lines) interactions.

required pump power $p_1 \approx |a_1|^2$ by the factor ω_3/ν is achieved; in the lower ionosphere this can be more than 2 orders of magnitude. The specific pump requirements for a steady state interaction relevant to ELF generation will be discussed in a later section.

As noted earlier, a key result due to *Reiman* [1977] for collisionless interactions is that if the threshold conditions (28) are satisfied, the linear stage of the absolute instability will be followed by pump depletion in the nonlinear stage. It has been shown that an absolute instability can also be established in the collisional regime. Furthermore, the pump threshold is much lower than in the collisionless case. This threshold reduction is of great practical interest, especially for applications to ELF generation. However, an equally important issue is whether the absolute instability would lead to pump depletion and, if so, what values of downconversion efficiency can be obtained. We demonstrate below that nonlinear saturation of absolute instabilities by pump depletion indeed occurs for collisional interactions and that downconversion efficiencies higher than those predicted by the Manley-Rowe relations can be reached.

The feature that distinguishes the collisional from the collisionless interaction is the presence of dissipative terms in the coupling coefficients so that the system's action and energy are no longer time invariant. To see this, we obtain from (24) the following relations for the one-dimensional space-time evolution:

$$\frac{\partial}{\partial t} S_{12} = - \int_{-\infty}^{\infty} dx \left[\Gamma_1 |a_1|^2 + \Gamma_2 |a_2|^2 + \frac{4\nu}{\omega_1} |K| \operatorname{Re} (a_1^* a_2 a_3) \right] \quad (38a)$$

$$\frac{\partial}{\partial t} S_{13} = - \int_{-\infty}^{\infty} dx \left[\Gamma_1 |a_1|^2 + \Gamma_3 |a_3|^2 - \frac{8\nu}{3\omega_3} |K| \operatorname{Re} (a_1^* a_2 a_3) \right] \quad (38b)$$

$$\frac{\partial}{\partial t} \Xi_T = - \int_{-\infty}^{\infty} dx \left[\omega_1 \Gamma_1 |a_1|^2 + \omega_2 \Gamma_2 |a_2|^2 + \omega_3 \Gamma_3 |a_3|^2 + \frac{4}{3} \nu |K| \operatorname{Re} (a_1^* a_2 a_3) \right] \quad (38c)$$

where

$$S_{12} = \int_{-\infty}^{\infty} dx [|a_1|^2 + |a_2|^2] \quad (39a)$$

$$S_{13} = \int_{-\infty}^{\infty} dx [|a_1|^2 + |a_3|^2]$$

$$\Xi_T = \sum_{j=1}^3 \Xi_j \quad \Xi_j = \int_{-\infty}^{\infty} dx \omega_j |a_j|^2 \quad (39b)$$

Notice that the value of $\int dx |a|^2$ is nothing more than the wave action (i.e., number of quanta). In the collisionless limit, the sums S_{12} and S_{13} of the actions and the total energy Ξ_T are time invariant. Equations (38) with zero on the right-hand side are commonly referred to as the Manley-Rowe relations. A direct consequence of these relations is the limitation on the downconversion efficiency from the pump (ω_1) to the signal (ω_3) to a value smaller than or equal to ω_3/ω_1 . Extensions of these results to the case of weakly dissipative systems with ponderomotive nonlinearity (i.e., $\Gamma_j/\omega_j \ll 1$) rely on the approximate conservation of S_{12} , S_{13} , and Ξ_T for them to be solvable by IST. The IST results have been compared with numerical solutions of (24) with $\nu = 0$ and found to agree. They give the same ω_3/ω_1 downconversion efficiency [*Liu*, 1976]. In order to examine the effect of the thermal nonlinearity we solve numerically the system of equations (24) with $\nu \neq 0$ but $\Gamma_j = 0$.

For the sake of simplicity, we limit ourselves to a model problem in one-dimensional space-time (x, t). As a comparison, the results for the collisionless interaction with symmetric coupling coefficients are also presented. The frequencies of the waves are chosen according to (11); for numerical convenience, we pick, in arbitrary units, $\omega_1 = 10.1$, $\omega_2 = 10.0$, $\nu = 1.2$, and $\omega_3 = 0.1$. The initial wave envelopes are rectangular, and the decay waves have small amplitudes; specifically, we let $|a_2|/|a_1| = 0.01$, $|a_3| = 0$. Because we have in mind an absolute instability, we also let the decay waves have opposite velocities $u_{3x} = -u_{2x}$, thus satisfying (28a). The problem is solved in the pump reference frame so that $u_{1x} = 0$. The pump threshold condition, (28b) or (37), is met by setting $|a_1| = 1.0$ in the collisionless case, whereas, in the collisional case, $|a_1| = |\Lambda|^{-1/2} = (4\nu/3\omega_3)^{-1/2} = 0.25$. With these values the respective normalized widths are the same, i.e., $L/l_c = L/l_c = 3.2$, so that from Figure 1a one expects a growing mode in both interactions.

Using the above initial conditions, the coupled system of equations (24) is numerically integrated forward in time. Figure 2 shows the time-asymptotic behavior at $t = 25.0$. We observe that pump depletion occurs in both interactions. In the collisionless case, the decay waves emerge as symmetric pulses. They are identified as solitons, as predicted by the IST solutions [*Kaup et al.*, 1979]. They are consistent with the Manley-Rowe relations, which predict an asymptotic state with $|a_2|/|a_3| \approx 1$ for pump depletion. On the other hand, the collisional interaction exhibits nonsymmetric pulses with $a_3 \gg a_2$, which suggests a rather different action transfer picture than that described by the Manley-Rowe relations. We have plotted in Figure 3 the percentage change of S_{12} and S_{13} with time. While there is a moderate decrease in S_{12} , the increase in S_{13} is dramatic. The preferential transfer of action to a_3 is understandable in view of the large factor ν/ω_3 in the low-frequency equation as compared to the small correction ν/ω_1 in the equation for a_2 . Physically, the enhancement is due to additional ω_3 photons that are being generated at a large rate via the temperature perturbation as a result of electron heating by the high-frequency waves. This is achieved at the expense of the total energy Ξ_T , which suffers a net loss to the medium as evident by the long-time decrease shown in Figure 3. In comparison, the corresponding collisionless interaction displays no noticeable change in any of the three quantities considered.

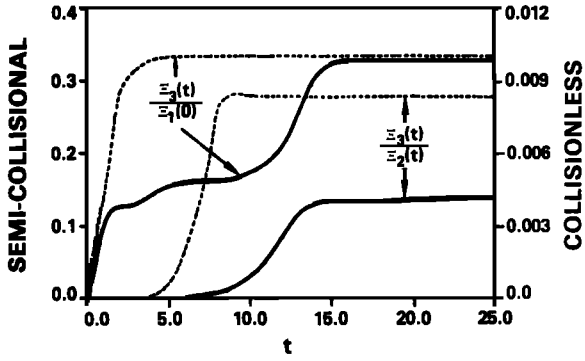


Fig. 4. The energy ratio $\Xi_3(t)/\Xi_1(0)$ and the downconversion efficiency $\Xi_2(t)/\Xi_1(t)$ versus time for the collisional (solid lines) and collisionless (dotted lines) interactions.

where we have used (25) and (27) for \tilde{u}_2 , \tilde{u}_3 , K , and \tilde{a}_1 in (42c). Recognizing

$$\frac{\partial D_j}{\partial k_{jx}} = -2k_{jx} \quad (45)$$

and substituting for β explicitly, we obtain

$$|E_1(z=0)| = \frac{4m_e c^2 \omega_1 \omega_{ce}}{e \omega_{pe}^2} \left| \frac{k_{2x}}{k_{3x}} \right| \left(\frac{L}{\tilde{l}_c} \right) \frac{1}{|\Lambda|^{1/2} L} \quad (46)$$

The requirement for absolute instability leading to complete decay is given by (42b). Therefore the threshold electric field found from (46) by taking $L/\tilde{l}_c \approx 2$ is

$$|E_1(z=0)|_{\text{THR}} = 400 \left(\frac{10 \text{ km}}{L} \right) \left(\frac{\omega_1 \omega_{ce}}{\omega_{pe}^2} \right) \left| \frac{k_{2x}}{k_{3x}} \right| \frac{1}{|\Lambda|^{1/2}} \text{ V/m} \quad (47)$$

For ionospheric conditions, $\omega_{ce} = 7.5 \times 10^6$ rad/s and $\nu = 2.5 \times 10^{-11} N T_e \text{ s}^{-1}$ based on ion-neutral collisions; N is in cm^{-3} and T_e in degrees Kelvin. Using these values, (47) can be written in practical units as

$$|E_1(z=0)|_{\text{THR}} = 22 \left(\frac{\omega_1}{\omega_{pe}} \right) \left| \frac{k_{2x}}{k_{3x}} \right| \left(\frac{10 \text{ km}}{L} \right) \left(\frac{10^5 \text{ cm}^{-3}}{n_0} \right)^{1/2} \cdot \left(\frac{10^{12} \text{ cm}^{-3}}{N} \right)^{1/2} \left(\frac{10^3 \text{ }^\circ\text{K}}{T_e} \right)^{1/2} \left(\frac{f_3}{100 \text{ Hz}} \right)^{1/2} \text{ V/m} \quad (48)$$

The power required to achieve this can be found from (48) by assuming that the HF illuminated region is a square with side L . Then

$$P_{\text{THR}} = \frac{1}{2} \epsilon_0 c |E_1(z=0)|_{\text{THR}}^2 L^2 \quad (49)$$

From (48) and (49) we find that in practical units,

$$P_{\text{THR}} = 64 \left(\frac{\omega_1}{\omega_{pe}} \right)^2 \left| \frac{k_{2x}}{k_{3x}} \right|^2 \left(\frac{10^5 \text{ cm}^{-3}}{n_0} \right) \left(\frac{10^{12} \text{ cm}^{-3}}{N} \right) \cdot \left(\frac{10^3 \text{ }^\circ\text{K}}{T_e} \right) \left(\frac{f_3}{100 \text{ Hz}} \right) \text{ MW} \quad (50)$$

The threshold power scales linearly with frequency, so that it is smaller for the lowest frequencies for which the analysis is applicable. The optimum interaction region height can be found by maximizing the product $n_0 N$. This is due to the weak dependence of the terms (ω_1/ω_{pe}) and (k_{2x}/k_{3x}) on the exact plasma parameters. We will further elaborate on these later on.

We proceed next to use the above equations in the design of a proof of principle ionospheric heating experiment. For con-

venience our estimates refer to the case where the magnetic field is perpendicular to the density gradient (Figure 5). This might not be the optimal case. Determination of the optimal geometry requires generalization of our calculation to include the effects of pump propagation between the ground and the interaction region, and the inhomogeneous structure of the pump near the reflection surface. These issues are currently under study and will be reported elsewhere. Before comparing the threshold conditions for the nonlinear interaction we examine the type of low-frequency waves of interest for our particular application. The dispersion relation for the low-frequency ionospheric modes was discussed in section 2. Referring to typical ionospheric conditions [Gurevich, 1978], we note that the ion-neutral collision frequency ν_3 is greater than $\omega_{ci} \approx 220$ rad/s for altitudes below 130 km, which is the region of interest in the present work. Therefore to excite low-frequency waves below 100 Hz, we must couple nonlinearly to the newly discovered helicon branch given by (7). As discussed in section 2, this branch occupies the range $\omega_3 < \nu_3$ and extends to very low frequencies. It is important to notice that contrary to the conventional situation, where the currents associated with the low-frequency waves are carried by the ions, in the helicon branch the currents are carried by the electrons. The ion dynamics is viscously frozen because of the high collisionality ($\nu_3 > \omega_{ci}$). Under these circumstances the Alfvén and magnetosonic modes are not proper eigenmodes.

Figure 5 is a schematic of the geometry in which two HF waves (ω_1, \mathbf{k}_1) , (ω_2, \mathbf{k}_2) interact nonlinearly in the ionosphere to drive a helicon with $\omega_3 < \nu_3$. The HF pump is incident at a small angle to \mathbf{B}_0 with a beam width equal to or smaller than the local density scale length L_n . For $\omega_1, \omega_2 \gg \omega_3$ the resonance conditions (11) yield a \mathbf{k}_3 that propagates almost directly downward. Such an interaction configuration can be achieved by grazing incidence of the HF beams at the desired ionospheric height (Figure 6).

Approximate values of the required power can be found from (50), by taking $k_{2x}/k_{3x} \approx 0.5$, $T_e \approx 10^3$ °K, and $\omega_1/\omega_{pe} \approx 2$. The value of $\omega_1/\omega_{pe} \approx 2$ implies a 30° incidence angle of the transmitter, which is sufficient to achieve long propagation paths [Ginzburg, 1970]. Using these values, (50) becomes

$$P_{\text{THR}} = 62 \left(\frac{10^5 \text{ cm}^{-3}}{n_0} \right) \left(\frac{10^{12} \text{ cm}^{-3}}{N} \right) \left(\frac{f_3}{100 \text{ Hz}} \right) \text{ MW} \quad (51)$$

Table 1 shows the power required to excite 100-Hz, 50-Hz, and 25-Hz waves as a function of height as computed by (51). The last column shows the required pump frequency versus height based on 30° incidence. Daytime conditions were assumed in compiling Table 1 [Gurevich, 1978]. Notice that the optimum interaction height is 100 km and relatively modest

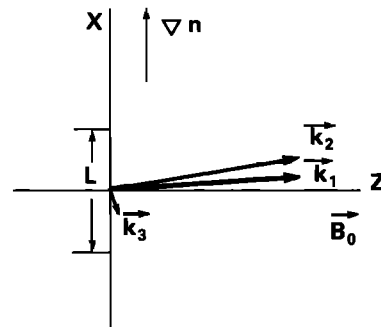


Fig. 5. Geometry of three-wave interaction in the lower ionosphere.

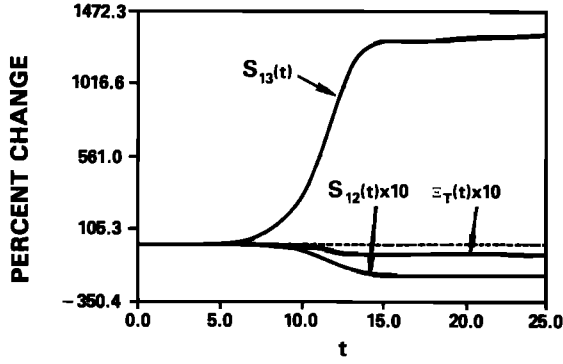


Fig. 3. Percentage change in the sums of the actions S_{12} , S_{13} and the total energy Ξ_T versus time. The dotted line indicates zero change for the collisionless interaction.

Of particular interest to the ELF/VLF generation is the efficiency with which one can downconvert the pump power into the low-frequency wave ω_3 . Toward this end, we have calculated the downconversion efficiency $\Xi_3(t)/\Xi_1(0)$ for both the collisional and collisionless interaction. Figure 4 shows an order-of-magnitude (~ 20) enhancement of the former over the latter. Also shown is the energy ratio $\Xi_3(t)/\Xi_2(t)$. Again we find that the collisional interaction assumes a much larger value (~ 0.8) at pump depletion. As the Manley-Rowe relations predict, the collisionless interaction yields a value equal to the frequency ratio $\omega_3/\omega_2 = 0.01$.

The present numerical results can be shown to be consistent with the action relations we previously derived. Subtracting (38a) from (38b) and integrating in time, we obtain ($\Gamma_j = 0$)

$$\int_{-\infty}^{\infty} dx (|a_3(t)|^2 - |a_2(t)|^2) = \frac{\nu}{\omega_3} \int_{-\infty}^{\infty} dx \sigma \quad (40a)$$

where

$$\sigma = \frac{2}{3} |K| \int_0^t dt \operatorname{Re} (a_1^* a_2 a_3) \quad (40b)$$

For the collisionless interaction ($\nu = 0$), (40a) simply states that the transfer of action to a_2 and that to a_3 are identical; hence the appearance of symmetric pulses in Figure 2. It then follows directly that the energy ratio in Figure 4 should be equal to ω_3/ω_2 , which it is. In the collisional case, (40a) implies a net gain in action transfer to a_3 , and we observe numerical evidence of this in the emergence of nonsymmetric pulses as well as in the increase in $\Xi_3(t)/\Xi_2(t)$. An expression for the downconversion efficiency may be obtained from (38b) by an integration in time ($\Gamma_j = 0$)

$$\frac{\Xi_3(t)}{\Xi_1(0)} = \frac{\omega_3}{\omega_1} \left\{ \int_{-\infty}^{\infty} dx \left[|a_1(0)|^2 - |a_1(t)|^2 + \frac{\nu}{\omega_3} \sigma \right] \right\} \cdot \left[\int_{-\infty}^{\infty} dx |a_1(0)|^2 \right]^{-1} \quad (41)$$

It is easy to see that in the collisionless limit, the maximum downconversion efficiency one can achieve is ω_3/ω_1 if the pump is completely depleted, i.e., $a_1(t) = 0$. In the example we consider, $a_1(t) \neq 0$, so that the downconversion efficiency is less than ω_3/ω_1 . The collisionless maximum ω_3/ω_1 , a consequence of the Manley-Rowe relations, can be exceeded in the collisional interaction when the collisional heating term dominates the pump depletion term, $|a_1(t)|^2$. Because of the large

factor ν/ω_3 , this may occur when the three waves overlap even over a short duration. As Figure 4 shows, the downconversion efficiency indeed exceeds ω_3/ω_1 without total depletion of the pump. Therefore we have the new interesting result that in a collisional interaction the Manley-Rowe relations no longer set the limit for the downconversion efficiency. The determining factor in this case is the cumulative collisional heating over time. The effect is most significant when the convection of the decay waves out of the pump is slow so that σ has the largest integrated value possible. Under such conditions the downconversion efficiency exceeds the collisionless maximum ω_3/ω_1 .

4. STEADY STATE INTERACTION: ELF GENERATION

Relevant to the ELF generation scheme is the steady state interaction given by (26). With the time variable replaced by z , the initial value problem we hitherto considered turns into a boundary value problem. The absolute instability found previously, which corresponds to an oscillator in time, now describes an amplifier in space for the low-frequency wave. In the nonlinear saturation stage, the pump depletes as it propagates. Because (24) and (26) are equivalent systems, it is straightforward to see that the conditions for absolute instability in the steady state case are

$$\tilde{u}_2 \tilde{u}_3 < 0 \quad (42a)$$

and

$$L > 1.8 \tilde{l}_c \quad (42b)$$

where

$$\tilde{l}_c = \frac{|\tilde{u}_2 \tilde{u}_3|^{1/2}}{|\tilde{K}^* \tilde{a}_1(z=0)| |\Lambda|^{1/2}} \quad (42c)$$

Since $u_{2z}, u_{3z} > 0$, (42a) coincides with (28a) while (42b) can be shown to be identical to (37), i.e., $\tilde{l}_c = l_c$, if one replaces the initial condition $a_1(t=0)$ in l_c by the boundary condition $\tilde{a}_1(z=0)$. It follows that the conclusions of the nonlinear analysis for the time-dependent case apply to the steady state interaction as well. Rather than energy, here one looks at the downconversion of HF power into the ELF/VLF signal. In analogy with (41), we can write the power downconversion efficiency out to a distance z as

$$\frac{P_3(z)}{P_1(0)} = \frac{\omega_3}{\omega_1} \left\{ \int_{-\infty}^{\infty} dx \left[|\tilde{a}_1(0)|^2 - |\tilde{a}_1(z)|^2 + \frac{\nu}{\omega_3} \sigma(z) \right] \right\} \cdot \left[\int_{-\infty}^{\infty} dx |\tilde{a}_1(0)|^2 \right]^{-1} \quad (43a)$$

where

$$P_j = \omega_j |\tilde{a}_j|^2 \quad (43b)$$

$$\sigma(z) = \frac{2}{3} |\tilde{K}| \int_0^z dz \operatorname{Re} (\tilde{a}_1^* \tilde{a}_2 \tilde{a}_3) \quad (43c)$$

Therefore, in the collisional limit, the amount of ELF power one can generate may exceed the collisionless maximum ω_3/ω_1 set by the Manley-Rowe relations, even when total pump depletion does not take place.

Of great practical interest to the ELF generation is the pump requirement for absolute instability. From the definition of \tilde{l}_c , we can solve for the incident pump field

$$|E_1(z=0)| = \frac{\omega_1}{|\beta|} \left| \frac{\partial D_2 \partial D_3}{\partial k_{2x} \partial k_{3x}} \right| \frac{1}{|\Lambda|^{1/2} \tilde{l}_c} \quad (44)$$

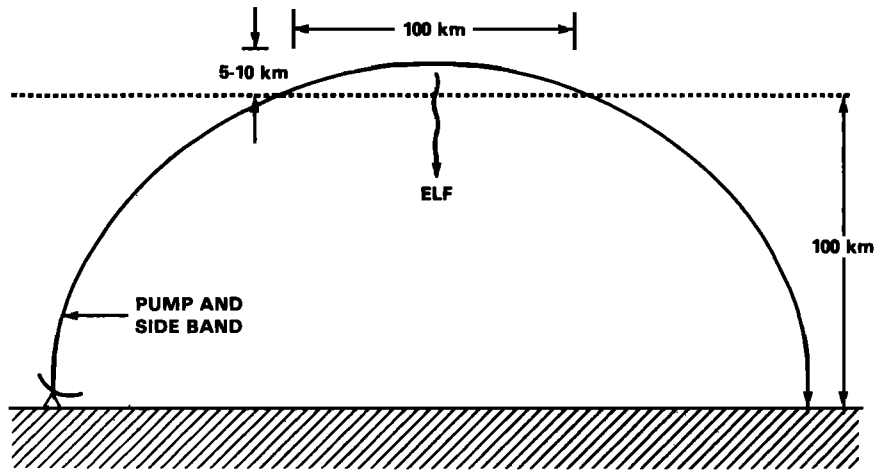


Fig. 6. Schematic of practical ELF generation scheme by grazing incidence of two HF heaters in the ionosphere.

power is required. We would like to stress that the values in Table 1 are indicative rather than exact. We feel that the assumption of $T_e \approx 10^3$ °K is very conservative and $T_e \approx 3-4 \times 10^3$ °K is more realistic. This will reduce the power requirement by factors of 3-4. On the other hand, a variety of propagation losses have been neglected. These will be considered in the future. It is interesting to note that $P_{THR} \sim (1/n_0) (1/N)$. Therefore further reduction in P_{THR} could be achieved if we could increase the local ionization by long-pulse radiation previous to the beat excitation.

5. SUMMARY AND CONCLUSIONS

We have examined stimulated excitation of ELF waves in the lower ionosphere by the use of two HF pumps. Previous work [Papadopoulos *et al.*, 1982, 1983] addressed the excitation of Alfvén and magnetosonic modes by similar techniques. However, since for ionospheric conditions, $v_3 \geq \omega_{ci}$ up to 150 km, excitation of these modes is possible only above that height. The thermal ponderomotive force driving the interaction is proportional to the electron-neutral collision frequency ν , which is by more than 2 orders of magnitude smaller above 150 km than near 100 km. The discovery that the helicon mode (C. R. Menyuk and K. Papadopoulos, private communication, 1984) is a proper eigenmode of the system even for frequencies with $\omega_3 < \nu_3$ allowed us to reduce the threshold for excitation of ELF waves below 100 Hz by more than 2 orders of magnitude, by coupling to the helicon mode in the vicinity of 100 km altitude. In addition to focusing on the helicon mode, a more detailed description was presented of the parametric decay processes in dissipative media discussed previously in a letter [Papadopoulos *et al.*, 1983]. As noted, a more comprehensive analysis including the

TABLE 1. Threshold Power for Excitation of 100-, 50-, and 25-Hz Waves Versus Ionospheric Heights

Height, km	P_{THR} , MW			f_1 , MHz
	100-Hz	50-Hz	25-Hz	
90	15	7.5	3.75	2.5
100	8	4	2	5
110	26	13	6.5	6
120	60	30	15	6.4

The last column gives the required pump frequency (based on equation (51)).

effects of oblique propagation of the pump from the ground to the ionosphere, the inhomogeneous structure of the pump in the interaction region, the inhomogeneous structure of the ionosphere, and a self-consistent description of the electron heating will be required to support proper experimental effort. Meanwhile the paper should be used as a guide to the physics expected during the interaction and the approximate design of ionospheric heaters required for a proof of principle experiment.

Before closing we should note that S. Ganguly and W. Gordon (private communications, 1984) reported preliminary evidence for beat wave generation for frequencies between 10 and 40 Hz, using the Arecibo HF facility. Their results were consistent with power threshold scaling increasing linearly with f_3 . The preliminary nature of the experimental results and the fact that the interaction region was in the *F* rather than the *E* region, where heat conditions, neglected in our analysis, dominate the energy transport, do not allow for a quantitative comparison of our theory with the experiment.

APPENDIX

The plane wave perturbations in a resonant three-wave interaction satisfy the fluid equations (8)–(10) as follows:

$$\mathbf{v} + \frac{i}{(\omega + i\nu)} \frac{e}{m_e} \left(\mathbf{E} + \frac{\mathbf{v} \times \mathbf{B}_0}{c} \right) \approx \frac{\mathbf{k}}{(\omega + i\nu)} \frac{T_0}{m_e} \left(\frac{T}{T_0} + \frac{n}{n_0} \right) - \frac{i}{(\omega + i\nu)} \left[\mathbf{v} \cdot \nabla \mathbf{v} + \frac{e}{m_e} \frac{\mathbf{v} \times \mathbf{B}}{c} + \frac{T_0}{m_e} \left(\frac{T}{T_0} - \frac{n}{n_0} \right) \frac{\nabla n}{n_0} \right]_{\omega, \mathbf{k}} \quad (\text{A1})$$

$$n - \frac{n_0 \mathbf{k} \cdot \mathbf{v}}{\omega} = - \frac{i[\nabla \cdot n\mathbf{v}]_{\omega, \mathbf{k}}}{\omega} \quad (\text{A2})$$

$$T - \frac{2}{3} \frac{T_0 \mathbf{k} \cdot \mathbf{v}}{(\omega + i\Delta\nu)} = - \frac{i}{(\omega + i\Delta\nu)} [\mathbf{v} \cdot \nabla T - \frac{2}{3} (\nu m_e \mathbf{v} - T\nabla) \cdot \mathbf{v}]_{\omega, \mathbf{k}} \quad (\text{A3})$$

The subscripts ω, \mathbf{k} for the square brackets indicate that the appropriate convolution product of the other two waves is taken to meet the matching conditions of (11). Equations (A1)–(A3) can be solved perturbatively.

Our main interest concerns the decay of a high-frequency electromagnetic pump wave (ω_1, \mathbf{k}_1) into a high-frequency sideband (ω_2, \mathbf{k}_2) and a low-frequency mode (ω_3, \mathbf{k}_3) in the

collisional regime. If we assume that the pump wave and its sideband have frequencies $\omega_{1,2} \gg \omega_{ce}$, the electrons are unmagnetized, and the left-hand sides of (A1)–(A3) yield, to lowest order, their driven velocities in the linear, cold limit,

$$\mathbf{v}_{1,2}^L \simeq -\frac{ie\mathbf{E}_{1,2}}{m_e\omega_{1,2}} \left(1 - \frac{iv}{\omega_{1,2}}\right) \quad (\text{A4})$$

By choosing the pump and sideband field polarizations as $\mathbf{E}_{1,2} = E_{1,2}\mathbf{y}$, we see from the left-hand sides of (A2) and (A3) the associated linear density and temperature perturbations vanish (in the (x, z) geometry), i.e.,

$$n_{1,2}^L = T_{1,2}^L = 0 \quad (\text{A5})$$

since the high-frequency waves are electromagnetic. For the low-frequency wave, the magnetized, cold, linear response as given by the left-hand sides of (A1)–(A3) is

$$\mathbf{v}_3^L = \frac{i\omega_3\boldsymbol{\epsilon}_3^e \cdot \mathbf{E}_3}{4\pi en_0} \quad (\text{A6})$$

$$n_3^L = \frac{n_0\mathbf{k}_3 \cdot \mathbf{v}_3^L}{\omega_3} \quad (\text{A7})$$

$$T_3^L = \frac{2}{3} \frac{T_0\mathbf{k}_3 \cdot \mathbf{v}_3^L}{(\omega_3 + i\Delta\nu)} \quad (\text{A8})$$

where $\boldsymbol{\epsilon}_3^e$ is the electron contribution to the cold plasma dielectric tensor.

At the next order, we evaluate the thermal and nonlinear terms on the right-hand sides of (A1)–(A3), using the lowest-order solutions, (A4)–(A8). It can easily be seen that there is no nonlinear modification to the density at all three frequencies (i.e., right-hand side of (A2) vanishes),

$$n_j^{\text{NL}} = 0 \quad j = 1, 2, 3 \quad (\text{A9})$$

whereas the nonlinear temperature perturbation is due only to ohmic heating,

$$T_j^{\text{NL}} = \frac{2}{3} \frac{ie}{(\omega_j + i\Delta\nu)} [vm_e v^2]_{\omega_j, \mathbf{k}_j} \quad (\text{A10})$$

Since the thermal pressure does not affect the electron velocities at high frequencies, we find, using (A1), the nonlinearly perturbed velocities

$$\mathbf{v}_{1,2}^{\text{NL}} = -\frac{ie\mathbf{E}_{1,2}^{\text{NL}}}{m_e(\omega_{1,2} + iv)} \quad (\text{A11})$$

where

$$\begin{aligned} \mathbf{E}_{1,2}^{\text{NL}} &= \frac{i\mathbf{k}_{1,2}T_{1,2}^{\text{NL}}}{e} + \left[\frac{m_e\mathbf{v}^L \cdot \nabla\mathbf{v}^L}{e} + \frac{\mathbf{v}^L \times \mathbf{B}}{c} \right]_{\omega_{1,2}, \mathbf{k}_{1,2}} \\ &\equiv \mathbf{E}_{1,2}^T + \mathbf{E}_{1,2}^P \end{aligned} \quad (\text{A12})$$

To arrive at (A11), we have combined the terms on the right-hand side of (A1) with the electric field term on the left-hand side and defined the nonlinear fields $\mathbf{E}_{1,2}^{\text{NL}}$ which contain, in addition to the ohmic heating, $\mathbf{E}_{1,2}^T$, the ponderomotive contributions within the square brackets, i.e., $\mathbf{E}_{1,2}^P$. In a similar fashion, the nonlinearly perturbed velocity at low frequency is given by

$$\mathbf{v}_3^{\text{NL}} = \frac{i\omega_3\boldsymbol{\epsilon}_3^e \cdot \mathbf{E}_3^{\text{NL}}}{4\pi en_0} \quad (\text{A13})$$

where

$$\mathbf{E}_3^{\text{NL}} = \frac{i\mathbf{k}_3 T_3^{\text{NL}}}{e} + \left[\frac{\mathbf{v}^L \times \mathbf{B}}{c} \right]_{\omega_3, \mathbf{k}_3} \equiv \mathbf{E}_3^T + \mathbf{E}_3^P \quad (\text{A14})$$

Here, the ponderomotive field is entirely due to the $\mathbf{E} \times \mathbf{B}$ drift of electrons. For our parameters of interest, the linear thermal pressure $n_0^L T_3$ turns out to be negligible and has been ignored.

The nonlinear current densities that drive the high-frequency waves ω_1, ω_2 are due to the nonlinearly perturbed velocities $\mathbf{v}_{1,2}^{\text{NL}}$ and to the beating of the linear velocities $\mathbf{v}_{1,2}^L$ with the low-frequency density perturbation n_3^L ,

$$\begin{aligned} \mathbf{J}_1^{\text{NL}} &= -e[n_0\mathbf{v}_1^{\text{NL}} + n_3^L\mathbf{v}_2^L] \\ \mathbf{J}_2^{\text{NL}} &= -e[n_0\mathbf{v}_2^{\text{NL}} + n_3^L\mathbf{v}_1^L] \end{aligned} \quad (\text{A15})$$

where the asterisk denotes the complex conjugate. We keep only the second of the two contributions to $\mathbf{J}_{1,2}^{\text{NL}}$ since it can be shown that its effect is greater by the ratio of high-frequency to low-frequency phase velocities. Expressing n_3^L , $\mathbf{v}_{1,2}^L$ explicitly in terms of the electric fields via (A4), (A6), and (A7), equations (A15) become

$$\begin{aligned} \mathbf{J}_1^{\text{NL}} &= -\frac{e}{4\pi m_e} \frac{\mathbf{E}_2}{\omega_2} \left(1 - \frac{iv}{\omega_2}\right) (\mathbf{k}_3 \cdot \boldsymbol{\epsilon}_3^e \cdot \mathbf{E}_3) \\ \mathbf{J}_2^{\text{NL}} &= \frac{e}{4\pi m_e} \frac{\mathbf{E}_1}{\omega_1} \left(1 - \frac{iv}{\omega_1}\right) (\mathbf{k}_3 \cdot \boldsymbol{\epsilon}_3^e \cdot \mathbf{E}_3)^* \end{aligned} \quad (\text{A16})$$

The low-frequency nonlinear current density, however, is caused solely by the nonlinearly perturbed velocity, i.e.,

$$\mathbf{J}_3^{\text{NL}} = -en_0\mathbf{v}_3^{\text{NL}} \quad (\text{A17})$$

because all high-frequency density perturbations vanish. The two nonlinear fields that drive \mathbf{v}_3^{NL} are evaluated separately. Substituting (A10) for T_3^{NL} , we have for the thermal field

$$\mathbf{E}_3^T = \frac{4}{3} vm_e \frac{\mathbf{k}_3}{\omega_3} \mathbf{v}_1^L \cdot \mathbf{v}_2^{L*} \quad (\text{A18})$$

where $\Delta\nu$ has been neglected when compared to ω_3 . If one replaces $\mathbf{v}_{1,2}^L$ by (A4), applies the frequency matching condition, and assumes $\omega_1 \sim \omega_2$, \mathbf{E}_3^T may be further reduced to

$$\mathbf{E}_3^T = -\frac{4}{3} \frac{ev}{m_e\omega_3} \frac{(\mathbf{E}_1 \cdot \mathbf{E}_2^*)}{\omega_1\omega_2} \mathbf{k}_3 \quad (\text{A19})$$

Similar treatment on the ponderomotive field

$$\mathbf{E}_3^P = \frac{\mathbf{v}_1^L \times \mathbf{B}_2^* + \mathbf{v}_2^{L*} \times \mathbf{B}_1}{c} \quad (\text{A20})$$

yields

$$\mathbf{E}_3^P = \frac{ie}{m_e} \frac{(\mathbf{E}_1 \cdot \mathbf{E}_2^*)}{\omega_1\omega_2} \left(\mathbf{k}_3 + \frac{i2v}{\omega_1} \mathbf{k}_1 \right) \quad (\text{A21})$$

where we have related $\mathbf{B}_{1,2}$ to $\mathbf{E}_{1,2}$ via Faraday's law and have made simplifications using vector identities. Dropping the contribution proportional to \mathbf{k}_1 because it is smaller in comparison to \mathbf{k}_3 , we finally obtain

$$\mathbf{J}_3^{\text{NL}} = \frac{e}{4\pi m_e} \frac{\omega_3}{\omega_1\omega_2} \boldsymbol{\epsilon}_3^e \cdot \mathbf{k}_3 (\mathbf{E}_1 \cdot \mathbf{E}_2^*) \left(1 + \frac{i4v}{3\omega_3}\right) \quad (\text{A22})$$

It is clear from (A22) that the thermal nonlinearity dominates when $v/\omega_3 \gg 1$, introducing an equivalent enhancement factor as well as a $\pi/2$ phase difference.

Acknowledgments. The authors wish to thank C. L. Chang, A. T. Drobot, and S. Ossakow for many helpful discussions. This work was supported by the U.S. Naval Research Laboratory contract N00014-82-M-0133.

The Editor thanks the two referees for their assistance in evaluating this paper.

REFERENCES

- Ablowitz, M. J., and H. Segur, *Solitons and the Inverse Scattering Transform*, Society for Industrial and Applied Mathematics, Philadelphia, Pa., 1981.
- Aigrain, P., in *Proceedings of the International Conference on Semiconductor Physics, Prague, 1960*, Academic, Orlando, Fla., 1961.
- Berger, R., M. V. Goldman, and D. Dubois, Stimulated diffusion scattering in ionospheric modification, *Phys. Fluids*, **18**, 207, 1975.
- Bobroff, L., and H. Haus, Impulse response of active coupled wave systems, *J. Appl. Phys.*, **38**, 390, 1967.
- Chang, C. L., V. Tripathi, K. Papadopoulos, J. Fedder, P. J. Palmadesso, and S. L. Ossakow, Wireless generation of ELF/VLF radiation in the ionosphere, in *Effect of the Ionosphere on Radiowave Systems*, edited by J. M. Goodman, p. 91, U.S. Government Printing Office, Washington, D. C., 1981.
- Ferraro, A. J., H. S. Lee, R. Allshouse, K. Carrol, A. A. Tomko, F. J. Kelly, and J. R. Joiner, VLF/ELF radiation from the ionospheric dynamo current system modulated by HF signals, *J. Atmos. Terr. Phys.*, **44**, 1113, 1982.
- Germantsev, G. G., N. A. Zuikov, N. A. Mityakov, and Ya. Y. Eidleman, Combination frequencies in the interaction between high-power short-wave radiation and the ionospheric plasma, *JETP Lett.*, Engl. Transl., **20**, 101, 1974.
- Ginzburg, V. L., *The Propagation of Electromagnetic Waves in Plasmas*, Pergamon, New York, 1970.
- Gurevich, A. V., *Nonlinear Phenomena in the Ionosphere*, Springer-Verlag, New York, 1978.
- Kapustin, I. N., P. A. Petrovskii, A. N. Yasil'ev, N. S. Smirnov, and O. M. Raspopov, Generation of radiation at combination frequencies in the region of auroral electrojet, *JETP Lett.*, Engl. Transl., **24**, 228, 1977.
- Kaup, D., A. Reiman, and A. Bers, Space-time evolution of nonlinear three-wave interactions, I, Interaction in a homogeneous medium, *Rev. Mod. Phys.*, **51**, 275, 1979.
- Krall, N., and A. Trivelpiece, *Principles of Plasma Physics*, McGraw-Hill, New York, 1973.
- Liu, C. S., Parametric instabilities in inhomogeneous unmagnetized plasma, *Adv. Plasma Phys.*, **6**, 83, 1976.
- Papadopoulos, K., and C. L. Chang, Generation of ELF/VLF waves in the ionosphere by dynamo processes, *Geophys. Res. Lett.*, **12**, 279, 1985.
- Papadopoulos, K., R. Sharma, and V. Tripathi, Parametric excitation of Alfvén waves in the ionosphere, *J. Geophys. Res.*, **87**, 1491, 1982.
- Papadopoulos, K., K. Ko, and V. Tripathi, Efficient parametric decay in dissipative media, *Phys. Rev. Lett.*, **51**, 463, 1983.
- Perkins, F. W., and M. W. Goldman, Self-focusing of radio waves in a underdense ionosphere, *J. Geophys. Res.*, **86**, 600, 1981.
- Reiman, A., Space-time evolution of nonlinear three-wave interactions, Ph.D. thesis, Princeton Univ., Princeton, N. J., 1977.
- Sagdeev, R., and A. Galeev, *Nonlinear Plasma Theory*, Benjamin, New York, 1969.
- Stamper, J. A., K. Papadopoulos, R. N. Sudan, S. O. Dean, E. A. McLean, and J. M. Dawson, Spontaneous magnetic fields in laser produced plasmas, *Phys. Rev. Lett.*, **26**, 1012, 1971.
- Stubbe, P., and H. Kopka, Modulation of the polar electrojet by powerful HF waves, *J. Geophys. Res.*, **82**, 2319, 1977.
- Stubbe, P., H. Kopka, and R. L. Dowden, Generation of ELF and VLF waves by polar electrojet modulation: Experimental results, *J. Geophys. Res.*, **86**, 9073, 1981.
- Stubbe, P., H. Kopka, H. Lauche, M. T. Rietveld, A. Brekke, O. Holt, and R. L. Dowden, Ionospheric modification experiments in northern Scandinavia, *J. Atmos. Terr. Phys.*, **44**, 1025, 1982a.
- Stubbe, P., H. Kopka, M. T. Rietveld, and R. L. Dowden, ELF and VLF wave generation by modulated HF heating of the current carrying low ionosphere, *J. Atmos. Terr. Phys.*, **44**, 1123, 1982b.
- Weiland, J., and H. Wilhelmsson, *Coherent Non-Linear Interaction of Waves in Plasmas*, Pergamon, New York, 1977.
- Zakharov, V., and S. Manakov, The theory of resonance interaction of wave packets in nonlinear media, *Sov. Phys. JETP*, Engl. Transl., **42**, 8421, 1975.

K. Ko and C. R. Menyuk, Science Applications International Corporation, 1710 Goodridge Drive; P. O. Box 1303, McLean, VA 22102.

P. Palmadesso, Naval Research Laboratory, Washington, DC 20305.

K. Papadopoulos, University of Maryland, College Park, MD 20742.

A. Reiman, Princeton Plasma Physics Laboratory, Princeton, NJ 08544.

V. Tripathi, Indian Institute of Technology, New Delhi 110016, India.

(Received May 2, 1986;
accepted May 2, 1986.)